Exhibit P

Alterations in Gene Expression in Human Mesothelial Cells Correlate with Mineral Pathogenicity

Arti Shukla[1]*, Maximilian B. MacPherson[1]*, Jedd Hillegass[1], Maria E. Ramos-Nino[1], Vlada Alexeeva[1], Pamela M. Vacek[2], Jeffrey P. Bond[3], Harvey I. Pass[4], Chad Steele[5], and Brooke T. Mossman[1]

Departments of [1]Pathology, [2]Medical Biostatistics, and [3]Microbiology and Molecular Genetics, University of Vermont College of Medicine, Burlington, Vermont; [4]Department of Cardiothoracic Surgery, NYU Langone Medical Center, New York, New York; and [5]Department of Medicine, University of Alabama at Birmingham School of Medicine, Birmingham, Alabama

Human mesothelial cells (LP9/TERT-1) were exposed to low and high (15 and 75 $\mu m^2/cm^2$ dish) equal surface area concentrations of crocidolite asbestos, nonfibrous talc, fine titanium dioxide (TiO_2), or glass beads for 8 or 24 hours. RNA was then isolated for Affymetrix microarrays, GeneSifter analysis and QRT-PCR. Gene changes by asbestos were concentration- and time-dependent. At low nontoxic concentrations, asbestos caused significant changes in mRNA expression of 29 genes at 8 hours and of 205 genes at 24 hours, whereas changes in mRNA levels of 236 genes occurred in cells exposed to high concentrations of asbestos for 8 hours. Human primary pleural mesothelial cells also showed the same patterns of increased gene expression by asbestos. Nonfibrous talc at low concentrations in LP9/TERT-1 mesothelial cells caused increased expression of 1 gene Activating Transcription Factor 3 (*ATF3*) at 8 hours and no changes at 24 hours, whereas expression levels of 30 genes were elevated at 8 hours at high talc concentrations. Fine TiO_2 or glass beads caused no changes in gene expression. In human ovarian epithelial (IOSE) cells, asbestos at high concentrations elevated expression of two genes (*NR4A2, MIP2*) at 8 hours and 16 genes at 24 hours that were distinct from those elevated in mesothelial cells. Since *ATF3* was the most highly expressed gene by asbestos, its functional importance in cytokine production by LP9/TERT-1 cells was assessed using siRNA approaches. Results reveal that *ATF3* modulates production of inflammatory cytokines (IL-1β, IL-13, G-CSF) and growth factors (VEGF and PDGF-BB) in human mesothelial cells.

Keywords: mesothelioma; crocidolite asbestos; talc; titanium dioxide; gene profiling

A myriad of natural and synthetic fibers and particles, including nanomaterials, are being introduced into the workplace and environment, and *in vitro* screening tests on human cell types are needed to predict their toxicity and mechanisms of action, especially in target cells of disease. Asbestos is a group of well-characterized fibrous minerals that are associated with the development of nonmalignant (asbestosis) and malignant (lung cancers, pleural, and peritoneal mesotheliomas) diseases in occupational cohorts (1–3), yet the molecular mechanisms of asbestos-related diseases are poorly understood. Although it is widely acknowledged that fibrous geometry, surface and chemical composition, and durability are important features in the development of asbestos-associated diseases, how these contribute to cell toxicity and transformation are unclear. Moreover, the early molecular events leading to injury by asbestos fibers and other pathogenic or innocuous particulates in human cells that may be targets for the development of disease remain enigmatic.

CLINICAL RELEVANCE

Results of work here suggest that transcriptional profiling can be used to reveal molecular events by mineral dusts that are predictive of their pathogenicity in mesothelioma.

The objective of work here was to compare acute toxicity and gene expression profiles of crocidolite asbestos, the type of asbestos most pathogenic in the causation of human mesothelioma (3, 4), to nonfibrous talc, fine titanium dioxide (TiO_2), and glass beads in a contact-inhibited, hTERT-immortalized human mesothelial cell line (5). In comparative studies, we also evaluated toxicity of particulates and gene expression changes in a contact-inhibited SV40 Tag-immortalized human ovarian epithelial cell line (IOSE) (6). This cell type is not implicated in asbestos-induced diseases, but is occasionally linked to inflammation and the development of ovarian cancer after use of talcum powder in the pelvic region, although such links are highly controversial (7).

Although most studies have evaluated the biological effects of particles and fibers on an equal mass or weight basis, the number, surface area, and reactivity of particulates at equal weight concentrations may be vastly different. Moreover, recent *in vitro* (8, 9) and *in vivo* (10–12), studies have confirmed that toxicity, oxidative stress, and inflammatory effects of ultrafine and other particles are related directly to surface area. For these reasons, and to avoid possible confounding alterations in gene expression or toxicity that might reflect or be masked in cells in different phases of the cell cycle, we introduced particulates at equal surface areas to confluent monolayers of human mesothelial (LP9/TERT-1) and human ovarian epithelial (IOSE) cells in a maintenance medium. Moreover, our studies included a nonfibrous talc sample and fine TiO_2 and glass particles, both traditionally used as nontoxic and nonpathogenic control particles in *in vitro* and animal experiments (reviewed in Refs. 13 and 14). Our studies provide novel insight into the early molecular events and responses occurring in human cells after exposure to asbestos and these materials.

MATERIALS AND METHODS

Human Mesothelial and Ovarian Epithelial Cell Cultures

Human mesothelial LP9/TERT-1 (LP9) cells, an hTERT-immortalized cell line phenotypically and functionally resembling normal human mesothelial cells (5), were obtained from Dr. James Rheinwald (Dana Farber Cancer Research Institute, Boston, MA). Human pleural mesothelial cells (NYU474) were isolated surgically from

(*Received in original form April 11, 2008 and in final form November 24, 2008*)

* These authors contributed equally to this research.

This work was supported by NIEHS training grant T32ES007122 to B.T.M., a contract from EUROTALC and the Industrial Minerals Association of North America, and NCI P01 CA 114,047 (H.I.P. and B.T.M.).

Correspondence and requests for reprints should be addressed to Arti Shukla, Ph.D., Department of Pathology, University of Vermont College of Medicine, 89 Beaumont Avenue, Burlington, VT 05405. E-mail: Arti.Shukla@uvm.edu

This article contains microarray data which can be found as a repository using the accession number GSE14034.

Am J Respir Cell Mol Biol Vol 41. pp 114–123, 2009 (1) Jul
Originally Published in Press as DOI: 10.1165/rcmb.2008-0146OC on December 18, 2008
Internet address: www.atsjournals.org

cancer-free patients by Dr. Harvey Pass (New York University, New York, NY). Briefly, tissue sample 2 × 2 cm^2 was harvested into saline solution and rinsed immediately with PBS (1×) and Dulbecco's modified Eagle's medium (DMEM) (1×). The tissue was then digested with 0.2% Collagenase type 1 (MP Biomedical Inc., Solon, OH) for 3 hours at 37°C. Finally, the digested tissue was scraped and cells collected were centrifuged for 5 minutes at 300 × *g*. The cell pellet thus obtained was resuspended in DMEM containing 10% fetal bovine serum (FBS) and 2% penicillin–streptomycin, transferred into 6-well plate, and allowed to grow at 5% CO_2 and 37°C. Mesothelial cells were characterized by staining with calretinin antibody. An SV40 Tag-immortalized, anchorage-dependent human ovarian epithelial cell line (IOSE 398) (6) was a kind gift from Dr. Nelly Auersperg (Canadian Ovarian Tissue Bank, University of British Columbia, Vancouver, BC, Canada). LP9/TERT-1 cells were maintained in 50:50 DMEM/F-12 medium containing 10% FBS, and supplemented with penicillin (50 units/ml), streptomycin (100 μg/ml), hydrocortisone (100 μg/ml), insulin (2.5 μg/ml), transferrin (2.5 μg/ml), and selenium (2.5 μg/ml). IOSE cells were maintained in 50:50 199/MCB105 medium containing 10% FBS and 50 μg/ml gentamicin. Cells at near confluence were switched to maintenance medium containing 0.5% FBS for 24 hours before particulate exposure. NYU474 cells were grown to near confluence in DMEM containing 10% FBS and supplemented with penicillin (50 units/ml) and streptomycin (100 μg/ml).

Characterization of Mineral Preparations

The physical and chemical characterization of the NIEHS reference sample of crocidolite asbestos has been reported previously (15). The surface area of asbestos fibers and particles was measured using nitrogen gas sorption analysis to allow computation of identical amounts of surface areas of particulates to be added to cells. Fiber and particle size dimensions were determined by scanning electron microscopy (SEM) as described previously (16). In addition, talc was examined using field emission scanning electron microscopy (FESEM) and transmission electron microscopy (TEM). The chemical composition, surface area, mean size, and source of each particulate preparation is presented in Table 1.

Introduction of Particulates to Cells

After sterilization under ultraviolet light overnight to avoid endotoxin and microbial contamination, particulates were suspended in HBSS at 1 mg/ml, sonicated for 15 minutes in a water bath sonicator, and triturated five times through a 22-gauge needle. This suspension was added to cells in medium.

SEM to Determine Particulate/Cell Interactions

Cells were grown on Thermonox plastic cover slips (Nalge Nunc International, Naperville, IL), exposed to particulates for 24 hours, and then processed for SEM as described previously (16). After samples were critical point-dried, they were mounted on aluminum specimen stubs and dried before being sputter-coated with gold and palladium in a Polaron sputter coater (Model 5100; Quorum Technologies, Guelph, ON, Canada) and examined on a JSM 6060 scanning electron microscope (JEOL USA, Inc., Peabody, MA).

Cell Viability Studies

After 24 hours, cells were collected with Accutase cell detachment reagent, and final cell suspensions in Accutase/complete medium/HBSS were mixed with 0.4% trypan blue stain, which is retained by dead cells. After 5 minutes, unstained cells were counted using a hemocytometer to determine the total number of viable cells per dish.

Based on the results of cell viability studies, asbestos and nonfibrous talc were evaluated in LP9 mesothelial cells for changes in gene expression at both low and high concentrations (15 and 75 $\mu m^2/cm^2$ dish) at 8 hours, and at low concentrations of minerals (15 $\mu m^2/cm^2$ dish) at 24 hours. These concentrations did not cause morphologic or toxic cellular changes at these time points. Negative control groups included cells exposed to fine TiO_2 (15 $\mu m^2/cm^2$ dish) at 8 and 24 hours and glass beads (75 $\mu m^2/cm^2$) at 24 hours. In IOSE cells, gene expression of all particulates was evaluated at 75 $\mu m^2/cm^2$ at 8 and 24 hours, as preliminary experiments revealed that no significant changes in mRNA levels were observed at 15 $\mu m^2/cm^2$ dish of asbestos. In NYU474 human mesothelial cells, QRT-PCR was used to validate a selected subset of gene expression changes identified by arrays in LP9/TERT-1 cells. Cells were exposed to 15 and 75 $\mu m^2/cm^2$ asbestos for 24 hours, and 8 genes highly expressed in LP9 cells were examined by QRT-PCR (*see below*).

RNA Preparation

Total RNA was prepared using an RNeasy Plus Mini Kit according to the manufacturers' protocol (Qiagen, Valencia, CA), as previously described (17).

Affymetrix Gene Profiling

Microarrays were performed on samples from three independent experiments. All cell types, time points, and mineral types and concenrations were included in all three experiments. For each experiment, $n = 3$ dishes were pooled into one sample per treatment group. Each of the pooled samples was analyzed on a separate array (i.e., $n = 3$ arrays per condition [3 independent biological replicates]). All procedures were performed by the Vermont Cancer Center DNA facility using standard Affymetrix protocol as previously described (14, 17). Each probe array, Human U133A 2.0 (Affymetrix, Santa Clara, CA) was scanned twice (Hewlett-Packard GeneArray Scanner, Palo Alto, CA), the images overlaid, and the average intensities of each probe cell compiled. Microarray data were analyzed using GeneSifter software (VizX Labs, Seattle, WA). This program used a "*t* test" for pairwise comparison and a Benjamini-Hochberg test for false discovery rate (FDR 5%) to adjust for multiple comparisons. A 2-fold cutoff limit was used for analysis.

Quantitative Real-Time PCR

Total RNA (1 μg) was reverse-transcribed with random primers using the Promega AMV Reverse Transcriptase kit (Promega, Madison, WI) according to the recommendations of the manufacturer, as described previously (17). In NYU474 mesothelial cells, eight genes (*ATF3*, *SOD2*, *PTGS2*, *FOSB*, *TFPI2*, *PDK4*, *NR4A2*, and *IL-8*) most highly expressed in LP9 cells were evaluated using the ΔΔCt method. Duplicate or triplicate assays were performed with RNA samples isolated from at least three independent experiments. The values obtained from cDNAs and hypoxanthine phosphoribosyl transferase (*hprt*) controls provided relative gene expression levels for the gene locus investigated. The primers and probes used to validate gene expression as observed in microarrays were purchased from Applied Biosystems (Foster City, CA).

TABLE 1. CHARACTERIZATION OF PARTICULATES

Name	Chemical Composition	Mean Surface Area ± SE (m^2/g)	Mean Size (μm)*	Source
Crocidolite Asbestos	$Na_2Fe_3^{2+}Fe_2^{3+}Si_8O_{22}(OH)_2$	14.97 ± 0.605	7.4 × 0.25	NIEHS Reference Sample
Talc (MP 10-52)†	$Mg_3Si_4O_{10}(OH)_2$	16.03 ± 0.654	1.1	Barrett's Minerals, Inc.
Titanium Dioxide	TiO_2	9.02 ± 0.185	0.69	Fisher Scientific
Glass Beads	SiO_2	2.78 ± 0.215	2.06	Polysciences Inc.

* Length X width for crocidolite asbestos, and diameter for nonfibrous talc, TiO_2, and glass beads.

† Although standard reference samples of asbestos and some particulates are available for use by the scientific community, reference samples of talc currently do not exist. For these reasons, the nonfibrous talc sample was also characterized for physical properties, particle size distribution (0.70 μm minimum to 1.20 μm maximum), and chemical/mineralogical (talc 95%, chlorite 4.5–5%, dolomite 0.3%) composition. For complete analysis or obtaining samples, please contact Brooke Mossman, Mark Ellis (markellis@ima-na.org), or Michelle Wyart at EUROTALC (mwyart@ima-europe.eu).

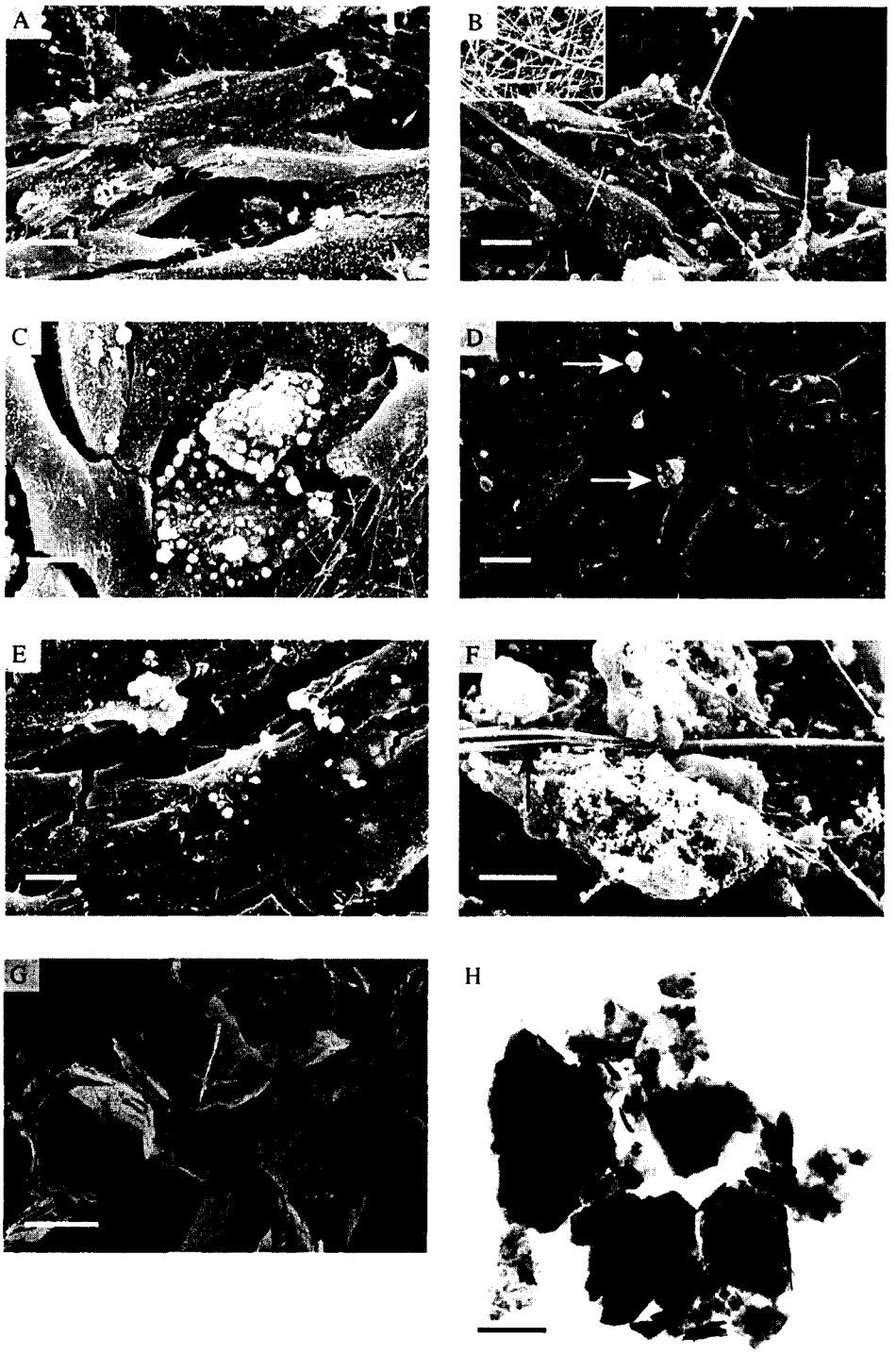

Figure 1. Interaction of fibers and particles with (*A–E*) LP9/TERT-1 human mesothelial cells and (*F*) IOSE ovarian epithelial cells after 24 hours of exposure to (*B, E, F*) high and (*C, D*) low concentrations of particulates. (*G*) Field emission scanning electron microscopy (FESEM) and (*H*) transmission electron microscopy (TEM) show structure of nonfibrous talc. (*A*) Morphology of unexposed near-confluent LP9/TERT-1 cells. (*B*) Membrane blebbing and piling up of cells in response to crocidolite asbestos (*arrows*). (*C*) Nonfibrous talc and (*D*) fine TiO_2 (*arrows*) on cell surface. (*E*) Single and small clumps of glass beads on plasma membrane. (*F*) Interaction of asbestos fibers (*arrows*) with IOSE cells that exhibit an exudate and membrane ruffling in response to fibers. *Bars* = 10 μm. (*G*) FESEM and (*H*) TEM showing morphology of platy talc bulk material. *Bars* = 2 μm.

Transfection of LP9 Cells with siRNA

On-Target plus Non-targeting siRNA #1 (scrambled control), and On-Target plus SMART pool human *ATF3* siRNA (100 nM; Dharmacon, Lafayette, CO) were transfected into LP9 cells at near confluence using Lipofectamine 2000 (Invitrogen, Carlsbad, CA), following the manufacturer's protocol. The efficiency of *ATF3* knockdown was determined by QRT-PCR after 48 and 72 hours.

Bio-Plex Analysis of Cytokine and Chemokine Concentrations in Medium of LP9/TERT-1 Cells

To quantify cytokine and chemokine levels in conditioned medium of cells transfected with siATF3 or scrambled control and exposed to asbestos for 24 hours, a multiplex suspension protein array was performed using the Bio-Plex protein array system as described previously (17) and a Human Cytokine 27-plex panel (Bio-Rad, Hercules, CA). Three biological replicates were used for each treatment group.

Statistical Analysis

Data from QRT-PCR and cell viability assays were evaluated by ANOVA using the Student Neuman-Keul's procedure for adjustment of multiple pairwise comparisons between treatment groups or using the nonparametric Kruskal-Wallis and Mann-Whitney tests. Differences with P values ≤ 0.05 were considered statistically significant.

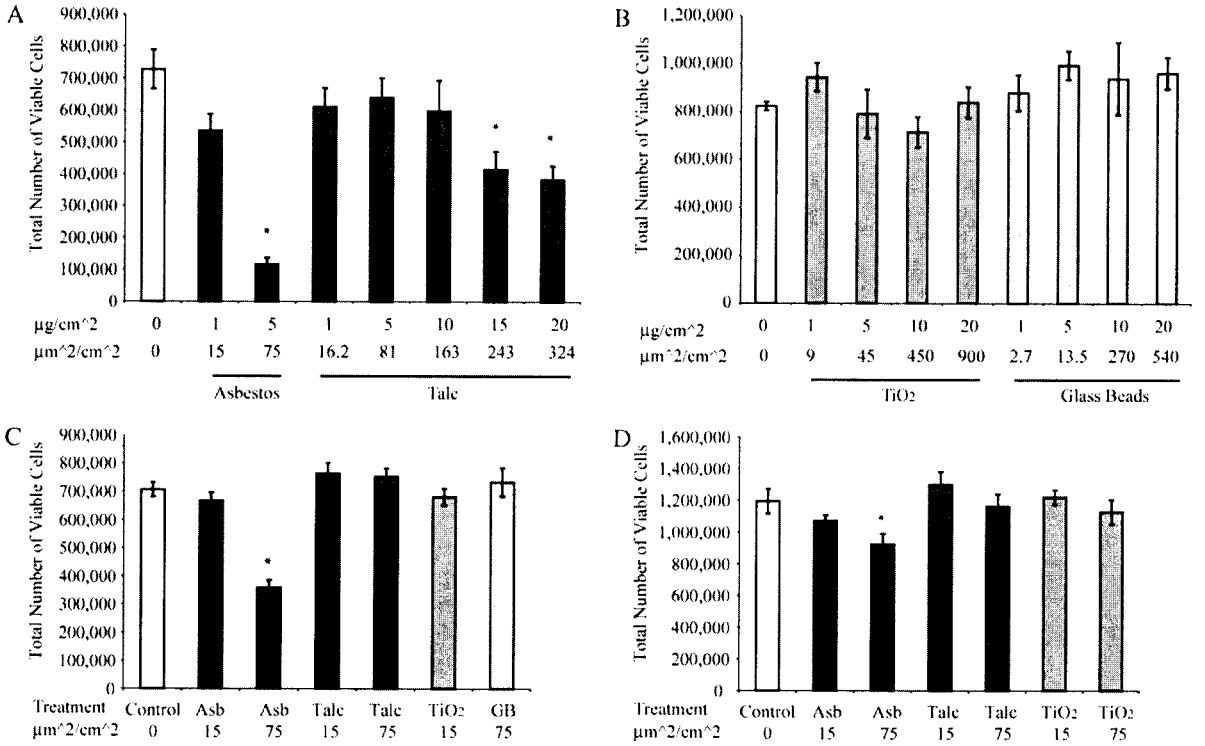

Figure 2. Cell viability after 24 hours of exposure to asbestos fibers and particles in (*A–C*) LP-9/TERT-1 and (*D*) IOSE (D). Mean +/− SE of 1 (A, B) or 3 (C, D) individual experiments where $n = 3$ per group per experiment. * $P \leq 0.05$ compared with untreated (0) groups.

RESULTS

Characterization of Particulate Preparations

Table 1 shows the major chemical formulas of crocidolite asbestos fibers (defined as having a greater than 3:1 length to width ratio) and particle samples used in experiments, although trace amounts of other elements occur in the NIEHS asbestos standards (15). In addition, we examined the morphology and cellular interactions of asbestos fibers, talc, and other particles using SEM (Figure 1). These studies revealed that only high (75 $\mu m^2/cm^2$) surface area concentrations of asbestos caused membrane blebbing and other toxic manifestations in cells (Figures 1B and 1F). In contrast, particles of nonfibrous talc (Figure 1C), fine TiO_2 (Figure 1D), and glass beads (Figure 1E) were nontoxic. Both asbestos fibers and particles were observed on the cell surface and were encompassed by cells. Nonfibrous talc occurred in platy particles that were uniform in appearance as viewed by FESEM (Figure 1G) and TEM (Figure 1H).

Asbestos Fibers at High Concentrations Are Toxic to LP9/TERT-1 Human Mesothelial Cells and Less So to Ovarian Epithelial Cells in Contrast to Particle Preparations

Figure 2 shows the results of trypan blue exclusion tests in LP9/TERT-1 and IOSE cells. In LP9/TERT-1 cells (Figures 2A–2C), asbestos at high surface area concentrations (75 $\mu m^2/cm^2$) caused significant decreases (50–80%) in cell viability that were more striking than those observed in IOSE cells (Figure 2D). Nonfibrous talc at 75 $\mu m^2/cm^2$ was nontoxic, and significant increases in toxicity were only achieved with addition of talc at ≥ 3-fold higher concentrations in LP9/TERT-1 cells (Figure 2A), but not in IOSE cells (data not shown). Neither TiO_2 nor glass beads were significantly toxic to either cell type over a range of concentrations (Figure 2B).

Asbestos Fibers, but Not Particle Preparations, Cause Dose- and Time-Related Changes in Gene Expression in Human LP9 Mesothelial Cells

Figure 3 shows a summary of significantly increased or decreased (> 2-fold compared with untreated controls) gene expression by asbestos (Figures 3A–3C) and nonfibrous talc (Figure 3D) in LP9/TERT-1 cells as well as the classification of genes by ontology. These studies revealed that gene expression changes by low concentrations of asbestos were less (29 increases) than at high concentrations (236 alterations including decreases) at 8 hours. Moreover, numbers of significant mRNA level alterations (205) at low concentrations of asbestos increased over time. In contrast, fewer numbers (30) of gene expression increases were observed at high concentrations of talc at 8 hours compared with identical surface areas of asbestos (236 changes), and no decreases in gene expression were observed. No significant alterations in gene expression were observed with low concentrations of talc at 24 hours or with TiO_2 or glass beads at either concentration or time point (data not shown). The major genes affected by asbestos or talc in LP9/TERT-1 cells are listed in Tables 2–4. This information reveals that the fold-increases in common genes expressed by asbestos-treated cells increase in a dose-related fashion at 8 hours. Although dose–responses were observed with talc at 8 hours, the numbers of significant gene increases as well as fold-increases were less than that observed with asbestos and decreased over time. Since mRNA expression of *ATF3* and *IL8* were increased by either asbestos or talc in LP9/TERT-1 cells, the increased expression of these genes was verified by QRT-PCR in mineral-exposed cells as compared with untreated control cells (Figure 4).

In NYU474 cells, QRT-PCR was used to validate that eight asbestos-induced genes in LP9 cells were up-regulated in

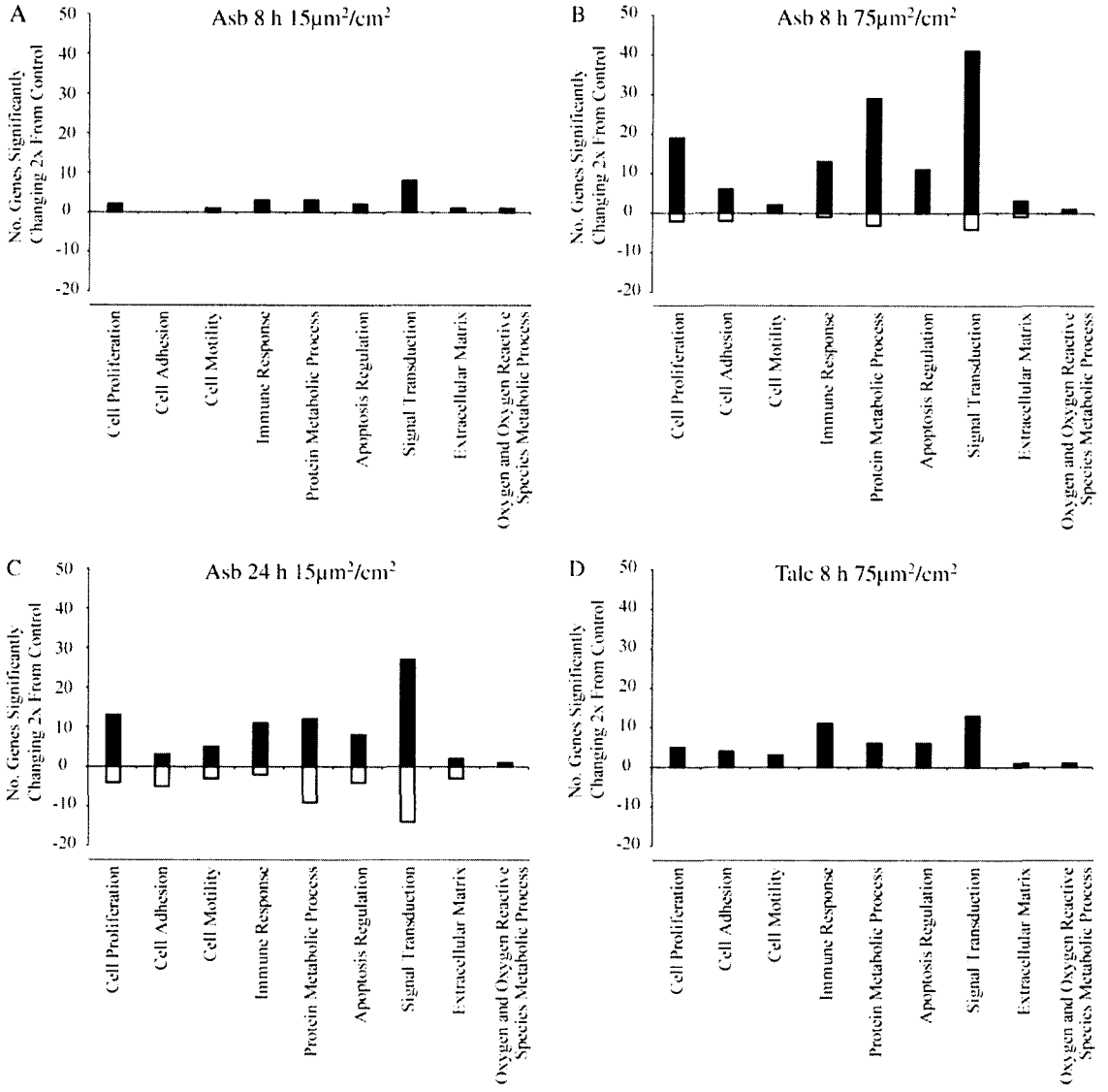

Figure 3. Numbers of changes ($P \leq 0.05$) in gene expression and classification by ontology in LP9/TERT-1 cells after exposure to (*A–C*) crocidolite asbestos or (*D*) nonfibrous talc.

normal human mesothelial cells (*ATF3*, *PTGS2* or *COX2*, *FOSB*, *IL8*, *NR4A2*, and *TFPI2*). Results showed that mRNA levels of six of the eight genes evaluated were increased in a dose-responsive fashion after exposure to asbestos for 24 hours (Figure 5).

IOSE Ovarian Epithelial Cells Exhibit Few Gene Expression Changes in Response to Asbestos

In contrast to LP9/TERT-1 and NYU474 mesothelial cells, IOSE cells showed no significant gene up-regulation or down-regulation in response to lower concentrations of asbestos at 8 or 24 hours (data not shown). At high concentrations of asbestos at 8 hours, mRNA levels of only two genes (*NR4A2* and *CXCL2* or *MIP2*) were increased in comparison to untreated IOSE cells (Table 4). At 24 hours, high concentrations of asbestos caused less than 4-fold increases in expression of only 16 genes, and decreased expression of 1 gene, *Profilin 1* (data not shown). No significant mRNA changes were observed with nonfibrous talc, fine TiO_2 or glass beads at either time point.

Inhibition of *ATF3* by siRNA Alters Asbestos-Induced Cytokines in LP9/TERT-1 Cells

Since *ATF3* was a common gene up-regulated by asbestos in mesothelial cells its functional role in cytokine production in LP9 cells was evaluated. As shown in Figure 6A, *ATF3* was successfully inhibited in LP9/TERT-1 cells using siATF3 as described in Materials and Methods. Cells transfected with control siRNA or siATF3 were then exposed to asbestos (75 $\mu m^2/cm^2$ $n = 3$) for 24 hours, and medium was collected and analyzed for cytokines and growth factors using Bio-Plex analyses. Inhibition of *ATF3* altered levels of asbestos-induced inflammatory cytokines (IL-1β, IL-13, G-CSF) and the growth factor (PGDF-BB) in LP9/TERT-1 cells (Figure 6B). Trends in diminishing levels of VEGF were also observed, although not statistically significant.

DISCUSSION

Gene expression analysis has been used for the classification of soluble toxicants in rodent and human cells *in vitro*. Models of

TABLE 2. TOP 10 GENES AFFECTED BY CROCIDOLITE ASBESTOS AT 8 AND 24 H IN LP9/TERT-1 HUMAN MESOTHELIAL CELLS

Concentration	Low ($15\ \mu m^2/cm^2$)		High ($75\ \mu m^2/cm^2$)
Time	8 h	24 h	8 h
	Fold Change		
Up-regulated			
Activating transcription factor 3 (*ATF3*)	9	9	27
Prostaglandin-endoperoxide synthase 2 (PTGS2)	7	8	16
Superoxide Dismutase 2 (SOD2)	6	6	2
Chemokine (C-X-C motif) ligand 3 (CXCL3)	4	NC	16
FBJ murine osteosarcoma viral oncogene homolog B (FOSB)	4	NC	NC
Tissue factor pathway inhibitor 2 (TFPI2)	4	14	11
Pyruvate dehydrogenase kinase, isozyme 4 (PDK4)	3	9	15
Chemokine (C-X-C motif) ligand 2 (CXCL2)	3	NC	NC
Angiopoietin-like 4 (ANGPLT4)	3	NC	NC
Kruppel-like factor 4 (gut) (KLF4)	3	NC	NC
Interleukin 8 C-terminal variant, 211506_s_t (IL8)	NC	8	12
Interleukin 1 receptor-like 1 (IL1R1)	NC	6	11
Nuclear receptor subfamily 4 (NR4A2)	NC	NC	11
Solute carrier family 7 (SLC7A2)	NC	6	10
Pleckstrin homology-like domain (PHLDA1)	NC	7	NC
Interleukin 8 (IL8)	NC	6	NC
Down-regulated			
Inhibitor of DNA binding 3 (ID3)	NC	NC	−5
Inhibitor of DNA binding 1 (ID1)	NC	NC	−3
Cytochrome P450, family 24 (CYP24A1)	NC	NC	−3
Basic helix-loop-helix domain (BHLHB3)	NC	NC	−3
SMAD family member 6 (SMAD6)	NC	NC	−3
S-phase kinase associated protein 2 (SKP2)	NC	NC	−3
Cadherin 10, type 2 (CDH10)	NC	NC	−3
START domain containing 5 (STARD5)	NC	NC	−3
211042_x_at	NC	NC	−2
Interferon-induced protein with tetratricopeptide (IFIT1)	NC	NC	−2
Oxytocin receptor (OXTR)	NC	−6	NC
Transcribed locus	NC	−5	NC
Chromosome 5 open reading frame (C5orf13)	NC	−5	NC
Cytochrome P450, family 24 (CYP24A1)	NC	−4	NC
Chromosome 21 open reading frame (C21orf7)	NC	−3	NC
KIAA1199	NC	−3	NC
Methyltransferase like 7A (METTL7A)	NC	−3	NC
PDZ domain containing RING finger 3 (PDZRN3)	NC	−3	NC
Periplakin (PPL)	NC	−3	NC
Phospholipase-C-like 1 (PLCL1)	NC	−3	NC

Definition of abbreviation: NC, no significant ($P \leq 0.05$) change > 2-fold from control.

transcript profiling for discrimination of toxic and nontoxic compounds in liver and other organs have also been developed in rodents (18), confirming the hypothesis that predictive modeling for classification of toxic agents and carcinogens is feasible. Here we used toxicogenomic approaches in human mesothelial cells, a cell type exquisitely sensitive to asbestos (19) and human contact-inhibited ovarian epithelial cells, a cell type not linked to carcinogenesis by asbestos, to determine whether the magnitude of altered gene expression by insoluble particulates correlated with their toxicity to cells and documented pathogenicity in humans. Although a recent study has examined gene expression profiles comparatively in crocidolite asbestos–exposed human lung adenocarcinoma (A549) and SV40-immortalized bronchial (BEAS-2B) or pleural mesothelial cell lines (MET5A) by cluster analysis (20), our studies are the first to examine gene expression changes by asbestos in comparison to other well-characterized particles in a human cell line that exhibits features of normal mesothelial cells (5). Although strict comparisons between cell types are not justified because SV40 Tag was used to immortalize the IOSE ovarian epithelial cell line (6), and SV40 infection is known to decrease sensitivity of human mesothelial cell lines to toxicity by asbestos (21), our studies suggest that the increased numbers of gene expression alterations observed in LP9/TERT-1 human mesothelial cells reflect elevated sensitivity of this cell type to asbestos. NYU474 human mesothelial cells were more resistant that LP9/TERT-1 cells to asbestos toxicity, permitting us to perform QRT-PCR studies at both concentrations of asbestos at 24 hours. These results confirmed common dose-related patterns of gene expression in mesothelial cells versus ovarian epithelial (IOSE) cells.

It is generally recognized that geometry and length and width (i.e., aspect ratio) of durable fibers such as amphibole asbestos types (crocidolite, amosite) are important properties determining toxicity, transforming potential, and carcinogeniciy in rodents and humans (13, 22, 23). Since talc can occur in various geometries (nonfibrous and fibrous) and can be contaminated with other minerals, including amphiboles, in some mining deposits (reviewed in Ref. 24), we used a well-characterized, nonfibrous talc sample here to allow evaluation of a particle not causing mesotheliomas or pleural sarcomas in rodents (23). Moreover, nonfibrous talc is regarded as noncarcinogenic in humans (25). Since talc is a magnesium silicate, and Mg^{2+} may interact with negatively charged molecules on the cell surface to

TABLE 3. GENES UP-REGULATED BY NONFIBROUS TALC IN LP9/TERT-1 HUMAN MESOTHELIAL CELLS

Gene	Fold Increase
8 h Low (15 $\mu m^2/cm^2$)	
Activating transcription factor 3 (*ATF3*)	3
8 h High (75 $\mu m^2/cm^2$)	
Activating transcription factor 3 (*ATF3*)	13
Inhibin, beta A (INHBA)	9
Chemokine (C-X-C motif) ligand 3 (CXCL3)	7
Superoxide dismutase 2 (SOD2)	7
Interleukin 8 C-terminal variant, 211506_s_t (IL8)	6
Prostaglandin-endoperoxide synthase 2 (PTGS2)	5
Interleukin 8 (IL8)	5
FBJ murine osteosarcoma viral oncogene homolog B (FOSB)	5
Tumor necrosis factor alpha-induced protein 6 (TNFAIP6)	4
Tissue factor pathway inhibitor 2 (TFPI2)	4
Chemokine (C-X-C motif) ligand 2 (CXCL2)	3
Intercellular adhesion molecule 4 (CICAM4)	3
ChaC, cation transport regulator homolog 1 (ChaC 1)	3
Nuclear receptor subfamily 4, group A, member 3 (NR4A3)	3
Pleckstrin homology-like domain, family A, member 1 (PHLDA1)	3
Interleukin 6 (IL-6)	3
Phorbol -12-myristate-13-acetate-induced protein 1 (PMA1P1)	3
Oxidized low density lipoprotein (lectin-like) receptor 1 (OLR1)	3
Chemokine (C-C motif) ligand 20 (CCL20)	3
v-maf musculoaponeurotic fibrosarcoma oncogene homolog F	3
Interleukin 1, alpha (IL-1α)	2
Tumor necrosis factor-α induced protein 3 (TNFA1P3)	2
Interleukin 1 receptor-like 1 (IL1RL1)	2
Angiopoieten-like 4 (ANGPLT4)	2
Kruppel-like factor 4 (KLF4)	2
GTP binding protein overexpressed in skeletal muscle (GEM)	2
Pentraxin-related gene, rapidly induced by IL-1 beta (PTX3)	2
Interleukin 1 beta (IL-1β)	2
HSPB (heat shock 27 kD) associated protein 1 (HSPBAP1)	2
Kynureninase (KYNU)	2

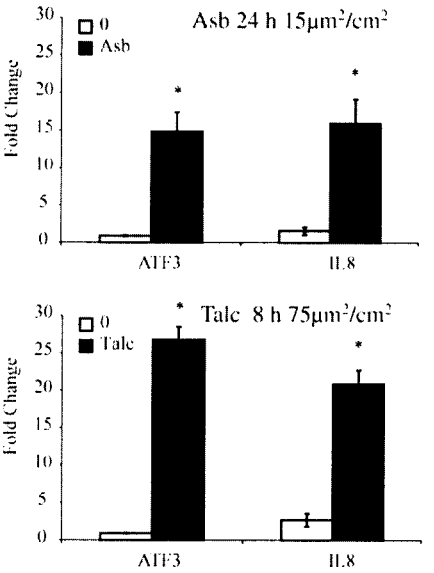

Figure 4. QRT-PCR confirms significant increases in *ATF3* and *IL8* expression by crocidolite asbestos at low concentrations and nonfibrous talc at high concentrations in LP9/TERT-1 mesothelial cells. *$P < 0.05$ as compared to untreated (0) groups.

disturb cell homeostasis (reviewed in Ref. 26), this may explain the few mRNA expression increases that were observed initially with talc at 8 hours. However, these changes were not observed at 24 hours, suggesting that human mesothelial cells adapt to or undergo repair after exposure to this mineral.

Our gene profiling data here and in inhalation studies using chrysotile asbestos (14) also support the concept that fine TiO_2 is nontoxic and nonpathogenic to mesothelial or other cell types. Likewise, in the rat, inhalation of fine TiO_2 (defined as particles > 0.1 μm in diameter), in contrast to ultrafine (particles < 0.1 μm in diameter) does not give rise to predictive markers of toxicity, inflammation, pulmonary fibrosis, or oxidative stress, as indicated by elevated levels of Mn-containing superoxide dismutase (*SOD2*) in cells from bronchopulmonary lavage (27). The increased reactivity and toxicity of ultrafine particles as compared with larger fine or coarse particles have also been confirmed in a number of *in vitro* and *in vivo* experiments and is often attributed to their increased surface area and/or ability to penetrate lung cells.

TABLE 4: GENES UPREGULATED BY CROCIDOLITE ASBESTOS IN IOSE HUMAN OVARIAN CELLS

Gene	Fold increase
8 h High (75 $\mu m^2/cm^2$)	
Nuclear receptor subfamily 4 (NR4A2)	4
Chemokine (C-X-C motif) ligand 2 (MIP2)	2
24 h High (75 $\mu m^2/cm^2$)	
Nuclear receptor subfamily 4 (NR4A2)	4
DNA-damage-inducible transcript 3 (DDIT3)	3
Stromal cell-derived factor 2-like 1(SDF2L1)	3
Heat shock 70 kD protein 1A (HSPA1A)	3
DnaJ (Hsp40) homolog, subfamily C (DNAJC3)	2
Paraspeckle component 1	2
Heat shock 70 kD protein 1B (HSPA1B)	2
Homocysteine-inducible, endoplasmic reticulum stress-inducible, ubiquitin-like domain member (HERPUD1)	2
Serum/glucocorticoid regulated kinase family, member 3 (SKG3)	2
DnaJ (Hsp40) homolog, subfamily B, member 9 (DNAJB9)	2
Arginine-rich, mutated in early stage tumors (ARMET)	2
Syntaxin 1A (brain) (STX1A)	2
Heat shock 70 kD protein 5 (HSPA5)	2
ADAM metallopeptidase with thrombospondin type 1 motif	2
Heat shock protein 90kDa beta (Grp94), member 1 (HSP90B1)	2

Our studies reveal a number of novel genes induced by asbestos in LP9/TERT-1 cells. As previously described in a lung epithelial cell line (C10) or mouse lungs after inhalation of crocidolite asbestos (28), increases in expression of the early response gene, *FOSB*, that encodes a dimer of the activator protein-1 transcription factor, were seen. Increases in expression of several other genes linked to cell signaling proteins and transcription factor activation were observed in asbestos-exposed cells, including *NR4A2* and *PDK4*. A novel gene up-regulated at all time points and concentrations of asbestos or talc in human mesothelial cells was activating transcription factor 3 (*ATF3*), a member of the cAMP-responsive element–binding (CREB) transcription factor family that encodes two different isoforms leading to repression or activation of genes. Silencing of *ATF3* in the present study by siRNA significantly altered expression of a number of asbestos-induced inflammatory cytokines and growth factors documented in malignant mesotheliomas (29, 30). In support of our results here, other studies using *ATF3*-deficient mice and *in vitro* approaches have shown that *ATF3* is a negative regulator of pulmonary inflammation, eosinophilia, and airway responsiveness (31). Moreover, *ATF3* also negatively regulates IL-6 gene transcription in an NF-κB model of up-regulation using melanoma cells (32). In addition, trends in production of VEGF, a known important angiogenic peptide and independent prognostic factor in human mesotheliomas (33), were observed. We have recently shown that an extracellular signal–related

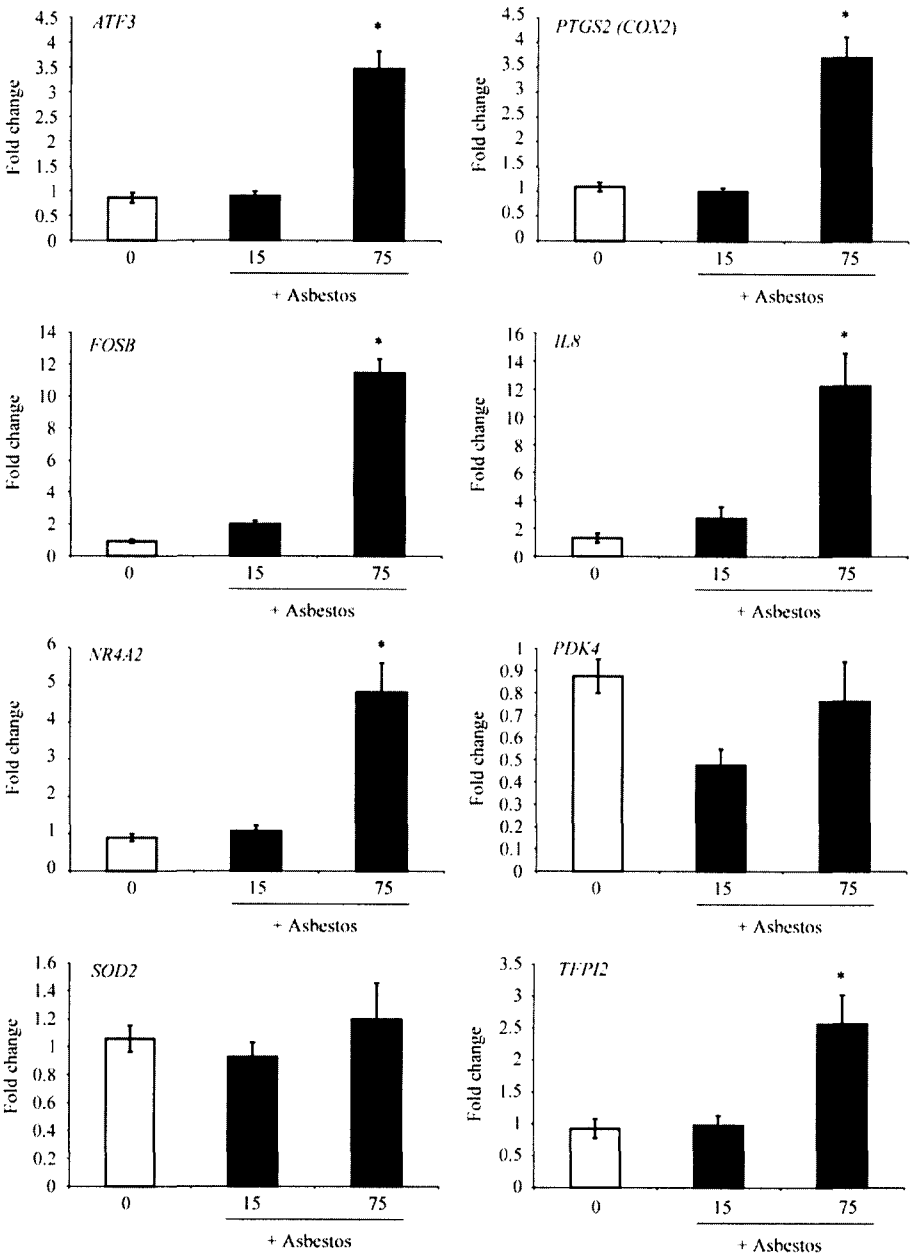

Figure 5. QRT-PCR confirms that human primary pleural mesothelial cells (NYU474) show similar patterns of asbestos-induced gene expression when compared with LP9/TERT-1 mesothelial cells. NYU474 cells were exposed to crocidolite asbestos (15 or 75 $\mu m^2/cm^2$) for 24 hours and cDNA was used for QRT-PCR. $^*P \leq 0.05$ as compared with untreated cells (0).

CREB pathway in C10 lung epithelial cells modulates apoptosis after asbestos exposure (34), and recent studies are focusing on the effects of silencing *CREB* or *ATF3* on other functional and phenotypic changes in human mesothelial and mesothelioma cells (A. Shukla and colleagues, unpublished data).

Several other genes up-regulated by talc at 8 hours or affected by asbestos at both 8 and 24 hours may be important in repair from mineral-induced responses. For example, *SOD2*, (Mn-containing superoxide dismutase) is an antioxidant protein occurring in the mitochondria, a target cell organ of asbestos-induced apoptosis (35). *PTGS2* (prostaglandin-endoperoxide syntase or cyclooxygenase) is a key enzyme in prostenoid biosynthesis associated with modulation of mitogenesis and inflammation. More recently, this pathway has been explored after interaction of ultrafine particles with alveolar macrophages (9). *ANG PTL4* (angiopoietin-4) encodes a serum hormone directly involved in regulating glucose homeostasis and lipid metabolism and is an apoptosis survival factor for vascular endothelial cells. The up-regulation of angiopoietin-4 is also thought to play a role in inhibition of tumor cell motility and metastasis. *KLF4* (Kruppel-like factor 4) is a negative regulator of cell proliferation and can be a positive or negative modulator of DNA transcription.

Increased expression of genes encoding different cytokines/chemokines (i.e., *IL8*) and their receptors or ligands (e.g., IL-8 C-terminal variant, *IL1R1*, *CXCL2* or *MIP2*, *CXCL3*, and *TFPI2*) by asbestos or talc suggests that the mesothelial cell also may play a role in chemotaxis, inflammation, and blood coagulation. A number of gene expression changes by asbestos also support the hypothesis that this fibrous mineral affects calcium-dependent processes including related protein kinase cascades, cell adhesion, and protein/lipid metabolism (Table 2). Although numbers of changes were more modest in IOSE cells, with the exception of *NR4A2* and *CXCL2*, a unique subset of genes was induced by asbestos in this cell type (Table 4).

Results of work here suggest that transcriptional profiling can be used to reveal molecular events by mineral dusts that are

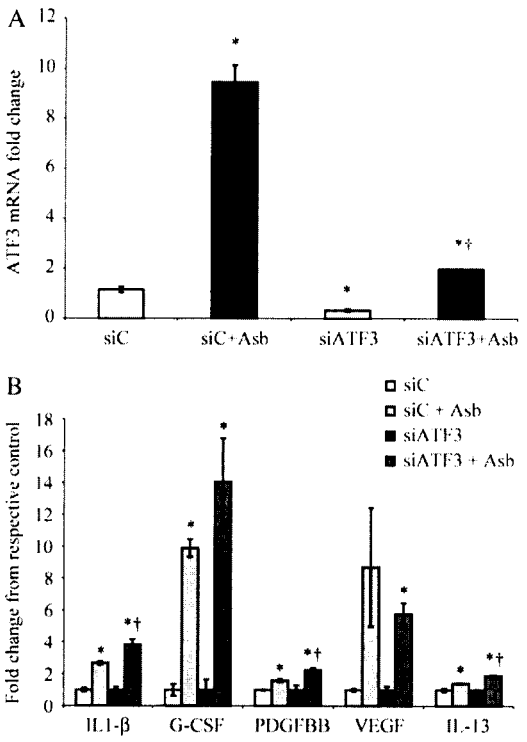

Figure 6. *ATF3* inhibition using siRNA approaches alters asbestos-induced production of inflammatory cytokines and growth factors. (*A*) LP9/TERT-1 cells transfected with siATF3 show significant inhibition of *ATF3* mRNA levels (untreated control [siC] versus siATF3 and asbestos-treated [siC Asb versus siATF3 Asb] groups). $^{*}P \leq 0.05$ as compared with siC; $^{\dagger}P \leq 0.05$ as compared with siC Asb group. (*B*) siATF3 altered asbestos-induced cytokine levels as detected in medium at 24 hours using Bio-Plex analyses. $^{*}P \leq 0.05$ as compared with control groups (siC and siATF3), respectively; $^{\dagger}P \leq 0.05$ as compared with asbestos-exposed scrambled control group (siC).

predictive of their pathogenicity in mesothelioma. Moreover, they reveal early and novel gene responses, including calcium-dependent transcription factors and antioxidant enzymes that may be pursued for their functional significance using RNA silencing or other approaches.

Conflict of Interest Statement: B.T.M. received support by EUROTALC and The Industrial Minerals Association (IMA) (11/1/05–10/31/06) for $90,000 for research. None of the other authors has a financial relationship with a commercial entity that has an interest in the subject of this manuscript.

Acknowledgments: The authors thank the Vermont Cancer Center DNA Analysis Facility for performing oligonucleotide microarray and real-time quantitative PCR, and Gary Tomiano (Minteg International, Inc./Specialty Minerals, Inc., Easton, PA) for talc characterization.

References

1. Mossman BT, Gee JB. Asbestos-related diseases. *N Engl J Med* 1989; 320:1721–1730.
2. Mossman BT, Churg A. Mechanisms in the pathogenesis of asbestosis and silicosis. *Am J Respir Crit Care Med* 1998;157:1666–1680.
3. Robinson BW, Lake RA. Advances in malignant mesothelioma. *N Engl J Med* 2005;353:1591–1603.
4. Mossman BT, Bignon J, Corn M, Seaton A, Gee JB. Asbestos: scientific developments and implications for public policy. *Science* 1990;247: 294–301.
5. Dickson MA, Hahn WC, Ino Y, Ronfard V, Wu JY, Weinberg RA, Louis DN, Li FP, Rheinwald JG. Human keratinocytes that express hTERT and also bypass a p16(INK4a)-enforced mechanism that limits life span become immortal yet retain normal growth and differentiation characteristics. *Mol Cell Biol* 2000;20:1436–1447.
6. Choi JH, Choi KC, Auersperg N, Leung PC. Overexpression of follicle-stimulating hormone receptor activates oncogenic pathways in pre-neoplastic ovarian surface epithelial cells. *J Clin Endocrinol Metab* 2004;89:5508–5516.
7. Merritt MA, Green AC, Nagle CM, Webb PM. Talcum powder, chronic pelvic inflammation and NSAIDs in relation to risk of epithelial ovarian cancer. *Int J Cancer* 2008;122:170–176.
8. Mossman BT, Shukla A, Fukagawa NK. Highlight Commentary on "Oxidative stress and lipid mediators induced in alveolar macrophages by ultrafine particles". *Free Radic Biol Med* 2007;43:504–505.
9. Beck-Speier I, Dayal N, Karg E, Maier KL, Schumann G, Schulz H, Semmler M, Takenaka S, Stettmaier K, Bors W, *et al.* Oxidative stress and lipid mediators induced in alveolar macrophages by ultrafine particles. *Free Radic Biol Med* 2005;38:1080–1092.
10. Oberdorster G, Ferin J, Gelein R, Soderholm SC, Finkelstein J. Role of the alveolar macrophage in lung injury: studies with ultrafine particles. *Environ Health Perspect* 1992;97:193–199.
11. Brown DM, Wilson MR, MacNee W, Stone V, Donaldson K. Size-dependent proinflammatory effects of ultrafine polystyrene particles: a role for surface area and oxidative stress in the enhanced activity of ultrafines. *Toxicol Appl Pharmacol* 2001;175:191–199.
12. Donaldson K, Tran CL. Inflammation caused by particles and fibers. *Inhal Toxicol* 2002;14:5–27.
13. Health Effects Institute - Asbestos Research. Asbestos in public and commercial buildings: a literature review and synthesis of current knowledge. Cambridge, MA: The Health Effects Institute; 1991.
14. Sabo-Attwood T, Ramos-Nino M, Bond J, Butnor KJ, Heintz N, Gruber AD, Steele C, Taatjes DJ, Vacek P, Mossman BT. Gene expression profiles reveal increased mClca3 (Gob5) expression and mucin production in a murine model of asbestos-induced fibrogenesis. *Am J Pathol* 2005;167:1243–1256.
15. Campbell WJ, Huggins CW, Wylie AG. Chemical and physical characterization of amosite, chrysotile, crocidolite, and nonfibrous tremolite for oral ingestion studies Washington, DC: National Institute of Environmental Health Sciences; 1980. No. 8542.
16. Blumen SR, Cheng K, Ramos-Nino ME, Taatjes DJ, Weiss DJ, Landry CC, Mossman BT. Unique uptake of acid-prepared mesoporous spheres by lung epithelial and mesothelioma cells. *Am J Respir Cell Mol Biol* 2007;36:333–342.
17. Shukla A, Lounsbury KM, Barrett TF, Gell J, Rincon M, Butnor KJ, Taatjes DJ, Davis GS, Vacek P, Nakayama KI, *et al.* Asbestos-induced peribronchiolar cell proliferation and cytokine production are attenuated in lungs of protein kinase C-delta knockout mice. *Am J Pathol* 2007;170:140–151.
18. Steiner G, Suter L, Boess F, Gasser R, de Vera MC, Albertini S, Ruepp S. Discriminating different classes of toxicants by transcript profiling. *Environ Health Perspect* 2004;112:1236–1248.
19. Lechner JF, Tokiwa T, LaVeck M, Benedict WF, Banks-Schlegel S, Yeager H Jr, Banerjee A, Harris CC. Asbestos-associated chromosomal changes in human mesothelial cells. *Proc Natl Acad Sci USA* 1985;82:3884–3888.
20. Nymark P, Lindholm PM, Korpela MV, Lahti L, Ruosaari S, Kaski S, Hollmen J, Anttila S, Kinnula VL, Knuutila S. Gene expression profiles in asbestos-exposed epithelial and mesothelial lung cell lines. *BMC Genomics* 2007;8:62.
21. Cacciotti P, Barbone D, Porta C, Altomare DA, Testa JR, Mutti L, Gaudino G. SV40-dependent AKT activity drives mesothelial cell transformation after asbestos exposure. *Cancer Res* 2005;65:5256–5262.
22. Davis JM, Addison J, Bolton RE, Donaldson K, Jones AD, Smith T. The pathogenicity of long versus short fibre samples of amosite asbestos administered to rats by inhalation and intraperitoneal injection. *Br J Exp Pathol* 1986;67:415–430.
23. Stanton MF, Layard M, Tegeris A, Miller E, May M, Morgan E, Smith A. Relation of particle dimension to carcinogenicity in amphibole asbestoses and other fibrous minerals. *J Natl Cancer Inst* 1981;67:965–975.
24. Guthrie GD Jr, Mossman BT. Health effects of mineral dusts. Washington, DC: Mineralogical Society of America; 1993.
25. IARC. Silica and some silicates. *IARC Monogr Eval Carcinog Risk Chem Hum* 1987;42:185.
26. Mossman B, Light W, Wei E. Asbestos: mechanisms of toxicity and carcinogenicity in the respiratory tract. *Annu Rev Pharmacol Toxicol* 1983;23:595–615.
27. Janssen YM, Heintz NH, Mossman BT. Induction of c-fos and c-jun proto-oncogene expression by asbestos is ameliorated by N-acetyl-L-cysteine in mesothelial cells. *Cancer Res* 1995;55:2085–2089.

28. Ramos-Nino ME, Heintz N, Scappoli L, Martinelli M, Land S, Nowak N, Haegens A, Manning B, Manning N, MacPherson M, *et al.* Gene profiling and kinase screening in asbestos-exposed epithelial cells and lungs. *Am J Respir Cell Mol Biol* 2003;29:S51–S58.
29. Yoshimoto A, Kasahara K, Saito K, Fujimura M, Nakao S. Granulocyte colony-stimulating factor-producing malignant pleural mesothelioma with the expression of other cytokines. *Int J Clin Oncol* 2005;10:58–62.
30. Vogelzang NJ, Herndon JE II, Miller A, Strauss G, Clamon G, Stewart FM, Aisner J, Lyss A, Cooper MR, Suzuki Y, *et al.* High-dose paclitaxel plus G-CSF for malignant mesothelioma: CALGB phase II study 9234. *Ann Oncol* 1999;10:597–600.
31. Gilchrist M, Henderson WR Jr, Clark AE, Simmons RM, Ye X, Smith KD, Aderem A. Activating transcription factor 3 is a negative regulator of allergic pulmonary inflammation. *J Exp Med* 2008;205:2349–2357.
32. Karst AM, Gao K, Nelson CC, Li G. Nuclear factor kappa B subunit p50 promotes melanoma angiogenesis by upregulating interleukin-6 expression. *Int J Cancer* 2009;124:494–501.
33. Demirag F, Unsal E, Yilmaz A, Caglar A. Prognostic significance of vascular endothelial growth factor, tumor necrosis, and mitotic activity index in malignant pleural mesothelioma. *Chest* 2005;128: 3382–3387.
34. Barlow CA, Barrett TF, Shukla A, Mossman BT, Lounsbury KM. Asbestos-mediated CREB phosphorylation is regulated by protein kinase A and extracellular signal-regulated kinases 1/2. *Am J Physiol Lung Cell Mol Physiol* 2007;292:L1361–L1369.
35. Shukla A, Stern M, Lounsbury KM, Flanders T, Mossman BT. Asbestos-induced apoptosis is protein kinase C delta-dependent. *Am J Respir Cell Mol Biol* 2003;29:198–205.